

# Advanced Controllers for Feed Drives

Y. Koren (1) and C. C. Lo

## SUMMARY

To achieve the high precision required in future contouring machining applications, accurate servo-controllers for the feed drives are needed. For this purpose conventional P controllers, which are utilized on many CNC systems, are not adequate, and more advanced control algorithms must be implemented. This paper summarizes existing servo-controllers for contouring applications and presents an evaluation of three basic types of controllers: feedback controller, feedforward controller, and cross-coupling controller. The evaluation of servo-controllers includes: (1) their abilities in eliminating different error sources and (2) their practical limitations in machine-tool control. The evaluation is supported by simulation and experimental results. In addition, some directions for future servo-control algorithms are also suggested.

**KEY WORDS:** Numerical control, machine tool, servo-controller.

## 1 INTRODUCTION

A general block diagram of a control loop used in machine tools is shown in Figure 1. In a typical machine tool system, each axis of motion is driven by a control loop. The controlled variable, which is the axial position, is fed back and compared with the reference input, which is the required axial position. The resulting error signal actuates the drive and motor through a controller so as to minimize, or eliminate, the position error. The simplest possible controller is one where the output signal is proportional to the error signal and is called the Proportional or P-controller.

There are two types of CNC systems: (1) point-to-point (PTP), and (2) contouring (or continuous-path). For PTP systems, a good axial positioning accuracy at the target points is required, and usually, a conventional P controller can satisfy this requirement [17,19] (note, however, that in high-friction machines, a PI controller is required). However, a conventional P controller may result in significant contour errors in machining contouring systems [18,19,35]. The term "contour error" is used to denote the error component orthogonal to the desired trajectory (i.e., the deviation of the cutter location from the desired path). The contour error in machining a desired contour on a two-axis system is shown in Figure 2. We should emphasize that the contour error, rather than the axial positioning error, is the prime concern, although the latter is usually given as the specification of CNC systems. Reduction of contour errors can be performed by three basic approaches: (1) applying more sophisticated axial controllers, (2) adding feedforward controllers, and (3) using a cross-coupling controller.

In the first approach, more comprehensive controllers than the P-controller are utilized (e.g., PID controller, state-feedback controller, etc.), and consequently, a reduction in the position errors of each individual axis is achieved

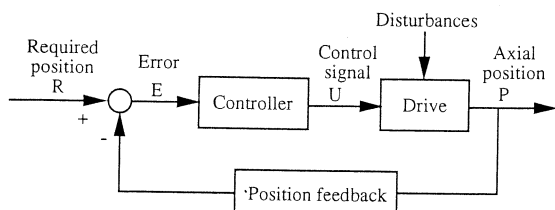


Figure 1: Block diagram of a control loop used in machine tools.

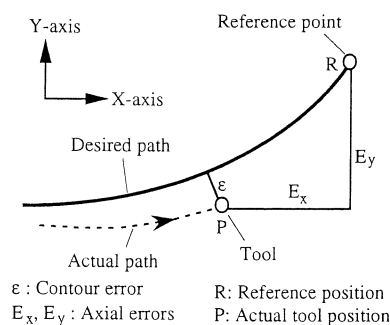


Figure 2: Contour error in machining a contour.

[4,12,15,28,32,36-38,56]. The second approach is based on adding a feedforward controller (e.g., ZPETC, IKF, etc.) to compensate for the axial position errors [14,16,20,29,30,32-34,40,42-48,50-52,54,55]. The above two approaches intend to *reduce the axial tracking errors* ( $E_x$  and  $E_y$  in Fig. 2) and thereby reduce the resultant contour error.

By contrast, the philosophy of the cross-coupling control method [8,11,18,22,24-27,31,50] is that the *elimination of the contour error* is the controller objective, rather than the reduction of the individual axial errors. Therefore, the cross-coupling concept calls for the construction of a contour-error model in real time and its utilization in the determination of a control law that reduces or eliminates the contour error.

Besides these three basic approaches, other control algorithms such as adaptive control [11,21,33,39-42,50], repetitive control [10,41,42,49,53], predictive control [5-7,13], and optimal control [1,25] may also be applied to improve the contouring performance of machine tool systems. These control algorithms could be considered as variations (e.g., optimal control, predictive control) or accessories (e.g., repetitive control, adaptive control) of these three basic servo-controllers.

The purpose of this paper is to discuss the above position servo-controllers and present a comparison of the three basic approaches (i.e., feedback, feedforward, and cross-coupling controllers). The evaluation of servo-controllers includes: (1) their abilities in minimizing or eliminating different error sources and (2) their limitations in machine tool control applications. The evaluation is supported by simulation and experimental results.

## 2 ERROR SOURCES

Contour error sources in machining may be classified into three categories: (1) mechanical hardware deficiencies (e.g., backlash, nonstraightness of the table, etc), (2) cutting process effects (e.g., tool deflection due to cutting force, tool wear, etc), and (3) controller and drive dynamics. The total dimensional error is a combination of all errors from the above sources. The first and second sets of error sources can be reduced by improving the mechanical hardware or utilizing compensation techniques, but cannot be reduced by the control techniques discussed in this paper. The third set of error sources, however, can be eliminated or reduced by improving the servo-control algorithms and is the main concern of this paper. These error sources are frequently overlooked by many machine tool builders, but they may be the dominant sources, especially in high-speed machining. Here we deal only with the contour error sources that are caused by the controller, drive dynamics, and external disturbances. These error sources can be further classified into three categories: (1) mismatch in axial-loop parameters, (2) external disturbances, and (3) the contour shape in nonlinear trajectories and corners.

### 2.1 Parameter Mismatch

A mismatch in axial-loop parameters causes contour errors. For example, in tracking a linear path, when using P controllers, a mismatch in the open-loop gains causes a steady-state contour error [18,19]

$$\epsilon_{ss} = \left( \frac{f_x f_y}{f} \right) \left( \frac{K_y - K_x}{K_x K_y} \right) \quad (1)$$

where  $K_x$  and  $K_y$  are the open-loop gains of the X- and Y-axis;  $f_x$  and  $f_y$  are the required velocities along the X- and Y-axis; and  $f$  ( $= \sqrt{f_x^2 + f_y^2}$ ) is the required feedrate (i.e., velocity) along the linear path. For example, if

$$K_x = 10 \text{ s}^{-1}, K_y/K_x = 1.03, f_x = f_y = 1.8 \text{ m/min} (= 71 \text{ ipm}),$$

then,  $\epsilon_{ss} = 62 \mu\text{m} (= 2.4 \text{ minch})$ .

The mismatch in time constants (i.e.,  $\tau_x \neq \tau_y$ ) in practical systems is usually more significant than that in the open-loop gains and, consequently, may cause a significant transient contour error, especially in high-speed cutting [39]. For example, if

$$K_x = K_y = 10 \text{ s}^{-1}, \tau_x = 40 \text{ s}, \tau_y = 50 \text{ s}, f_x = f_y = 1.8 \text{ m/min} (= 71 \text{ ipm})$$

then,  $\epsilon_{\max} = 105 \mu\text{m}$ . (Calculated by a simulation in which the sampling period = 0.01 sec).

## 2.2 Disturbances

A disturbance in control loops means an external action to the loop that changes or disturbs the desired operation of the controlled variable. The controlled variable in our case is the tool position relative to the part. The load disturbances include the friction of the machine guides and the cutting forces. There are two types of friction: Coulomb friction and viscous friction. The former is usually modeled as a step disturbance where its direction is always opposite to the motion. The latter is a function of the feedrate and increases as the feedrate increases [9]. Only Coulomb friction is considered in this paper.

The cutting force  $F$  is a function of the feed  $s$  and the depth of cut  $a$  [3,23].

$$F = K_s s^\alpha a^\beta \quad (2)$$

Typical values are  $\alpha = 0.73$  and  $\beta = 1$ . The relationship between the feed  $s$  and the feedrate  $f$  is

$$f = p s N \quad (3)$$

where  $N$  is the spindle speed and  $p$  is the number of teeth in the milling cutter (in turning  $p = 1$ ).

The cutting force is a vector. Equation 2 shows the magnitude of the cutting force. The direction of the cutting force, however, is not determined by Equation 2. In slot milling or in end milling with constant depth of cut, the cutting force has a constant angle to the tangent of the direction of the cutting force (see Fig. 3), and this determines the direction of the cutting force [3].

Combining the Coulomb friction and the cutting forces, the disturbance loads consist of a step component, which is always opposite to the motion, and a trajectory-dependent component with a magnitude that is a function of the feedrate (assuming that  $N$  is constant). The axial load disturbances used in the simulations are described in Figure 3 and given in the following equations:

$$D_x = D_{fx} \text{sign}(f_x) + D_C \cos(\phi - \theta) \quad (4)$$

$$D_y = D_{fy} \text{sign}(f_y) - D_C \sin(\phi - \theta)$$

$$\text{where } D_C = K_c f^{0.73}$$

where  $\text{sign}()$  is the signum function,  $D_{fx}$  and  $D_{fy}$  are the disturbances caused by Coulomb friction (in the simulation we assume  $D_{fx} = D_{fy}$ ),  $D_C$  is the disturbance caused by the cutting force,  $\theta$  is the angle between the tangent of the desired trajectory and the X-axis, and  $\phi$  is the angle between the resultant cutting force and the tangent of the desired trajectory.

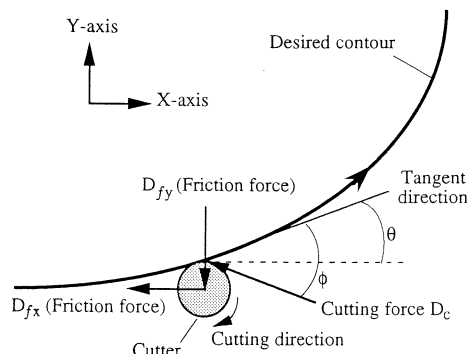


Figure 3: The disturbance model used in simulations.

For machining a linear contour when utilizing a P controller, the steady-state contour error caused by the above disturbances is given by the following equation [18]:

$$\epsilon_{ss} = \frac{f_y D_x - D_y f_x}{\tau(1-e^{-T/\tau})K_p f} \quad (5)$$

where  $\tau$  is the open-loop time constant,  $T$  is the sampling period, and  $K_p$  is the P-controller gain.

## 2.3 Contour Shape

When producing a linear contour, each axis receives a position ramp input as a reference. The slope of the ramp is proportional to the required axial velocity. For ramp inputs, the control loop does not need special tracking abilities. When producing nonlinear contours, however, the inputs to the control loops are also nonlinear. For example, in order to produce the circle

$$(x - \rho)^2 + y^2 = \rho^2,$$

where  $\rho$  is the radius of the circle, the inputs to the control loops are

$$x = \rho(1 - \cos\omega t)$$

$$y = \rho \sin\omega t$$

where  $\omega = f/\rho$  and  $f$  is feedrate along the circle. It is known that in response to these inputs each axial motor will have initial transients and then move in a sinusoidal motion with the same angular velocity  $\omega$ , but with a phase shift. Both the phase shift and motion amplitude of the motors are function of  $\omega$ . Therefore the contour error is also a function of  $\omega$ .

For a matched second order system, Poo and Bollinger [35] formulate the steady-state contour (or radial) error in a circular motion in the following:

$$\frac{\epsilon_{ss}}{\rho} = 1 - \frac{1}{\sqrt{1 + (2\zeta\omega/\omega_n)^2 - 2(\omega/\omega_n)^2 + (\omega/\omega_n)^4}} \quad (6)$$

where  $\zeta$  and  $\omega_n$  are the control loop damping factor and natural frequency, respectively. (Note that  $f = \rho\omega$ .)

Similar errors occur for other types of nonlinear shapes such as ellipses, parabolas or high-order splines. Another type of contour error occurs in cutting sharp corners [19]. For example, if the table moves only in the X-direction before the corner, and then in the Y-direction, the X-axis will still move when the Y motion starts, which causes a contour error.

## 2.4 Conclusions

As shown in Equations 1-6, the error due to all sources, except the Coulomb friction, increases as the feedrate increases. Our intermediate conclusions are the following. (1) The contour error is amplified by the feedrate. Since the feedrate is proportional to the spindle speed (see Eq. 3), and the latter is proportional to the cutting speed, the contour error is amplified by the cutting speed. Therefore, a more effective servo-controller (in terms of error reduction) is needed for systems that utilize high-speed machining. (2) For the machine tool systems with large Coulomb friction, an effective servo-controller is needed even at low cutting speeds.

## 3 FEEDBACK CONTROLLERS

All the controllers of machine tools have feedback. The term "feedback controller" here means a controller that uses only basic feedback principles. In CNC these controllers may be classified into three basic classes: P, PID, and state-feedback controllers.

### 3.1 P Controller

Proportional (P) controller is the most conventional feedback controller in CNC. It sends correction signals proportional to the difference between the reference position and the actual position. The proportional gain, is usually designed so that the closed loop damping ratio ( $\zeta_{\text{closed}}$ ) is equal to 0.707. For this damping ratio, the following equation can be used for the selection of the proportional open-loop gain [17].

$$K_{\text{open}} = \frac{1}{T + 2\tau} \quad (7)$$

where  $T$  is the sampling period,  $\tau$  is the open-loop time constant, and  $K_{\text{open}}$  is the open-loop gain, which is the product of the P-controller gain ( $K_p$ ) and the other gains in the system such as motor's gain ( $K_m$ ), gear ratio ( $K_g$ ), encoder gain ( $K_e$ ), etc.

For conventional feedrates (e.g., 0.25 m/min = 10 ipm) and small disturbance loads, this controller gives reasonable contour errors (e.g., 0.01 mm), and the dominate sources for dimensional errors on the parts are other than the servo errors (e.g., machine geometry, machine temperature, and tool deflection).

### 3.2 PID Controller

In a PID controller, the correction signal is a combination of three components: a proportional, an integral, and a derivative of the position error. The task of the integral (I) controller is to eliminate the steady-error when position ramp inputs are the references, as in the case of linear cuts, and to reject the external disturbances. However, implementing an I-controller by itself will cause instability, and it must be combined with a proportional action to enable a stable system. The derivative (D) controller aids in shaping the dynamic response of the system. The combination is known as a PID controller. Since a computer is utilized as the controller, a digital PID is implemented.

There are different ways to design digital PID controllers. We can, for example, formulate the digital PID controller law by approximating the continuous-time PID controller with backward difference or Euler's or Tustin's methods [1]. In the following analyses, the PID controller law ( $H_x(z)$  and  $H_y(z)$  for X- and Y-axis, respectively) is formulated based on backward difference approximation, using z-transform

$$H_x(z) = H_y(z) = K_P + K_I \frac{Tz}{z-1} + K_D \frac{z-1}{Tz} \quad (8)$$

where  $K_P$ ,  $K_I$ ,  $K_D$  are the proportional, integral, and derivative gains, respectively. The integral gain  $K_I$  is chosen large enough to guarantee a good ability in disturbance rejection, and the derivative gain  $K_D$  is designed to guarantee small overshoot. Usually, the controller gains can be designed based on root locus or frequency domain methods.

The two main problems with PID controllers in contouring application are (1) poor tracking of corners and nonlinear contours (see Section 7.1 below) and (2) significant overshoots. To reduce the effect of these problems, the gain  $K_I$  should be small and the implementation of the controller requires careful preprogramming of acceleration and deceleration periods, whereas these are not needed with a P controller.

In addition to the basic PID shown in Figure 4a, some different PID-structures, shown in Figures 4b, 4c, and 4d, were applied in practical servo-controllers [1,28,36-38,56]. However, since Figure 4a represents the most common structure, it is used in the analyses and simulations in this paper.

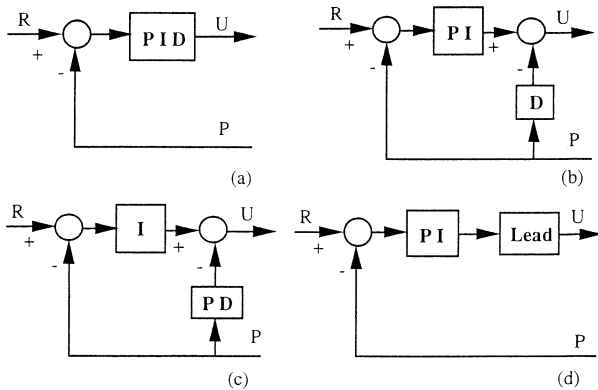


Figure 4: Different ways to implement controllers with PID functions.

### 3.3 State-Feedback Controller

The most common measurable states in CNC are the position and the velocity. The axial position is measured by an incremental encoder and an associated counter, and the velocity may be measured either by a tachometer [19,28] or by differentiating the measured position [36-38,56]. The velocity closed loop, however, can be either closed in hardware [19,28] or in the computer [36-38,56]. If the feedback states are the position and the velocity, the state-feedback controller is in fact a PD-controller (shown in Figure 4b without the integral action). However, to eliminate the steady-state error, the state-feedback controller can also implement the integral control by augmenting the state vector with an

extra state representing the integral of the output error. The state-feedback controller then is similar to a PID controller, and therefore, it will not be further discussed in this paper.

## 4 FEEDFORWARD CONTROLLERS

To decrease the tracking errors, feedforward controllers might be added to the control loops. We discuss below two basic types and two improved feedforward controllers.

### 4.1 Basic Feedforward Controllers

There are two principal types of feedforward controllers, which are shown in Figure 5. The principle of the design in Figure 5a [14,16,30,40,42,45-48,51,52,54,55] is simple: implement in the control computer a transfer function  $G_0^{-1}(z)$  that is the exact inverse of the one of the real control loop,  $G(z)$ , i.e.,  $G_0^{-1}(z)G(z) = 1$ , and then the actual position becomes equal to the required position.

The design in Figure 5b has the same objective [20,29,32,34]. If we implement an inverse transfer function of the drive unit in the feedforward controller block, as shown in Figure 5b, we obtain the following closed-loop equation:

$$\frac{P}{R}(z) = \frac{D_0^{-1}(z)D(z) + H(z)D(z)}{1 + H(z)D(z)} \quad (9)$$

where  $H(z)$  and  $D(z)$  represent the transfer functions of the software controller and the drive unit, respectively. If  $D_0(z) = D(z)$ , the overall relation between the required position and the actual position becomes 1:1.

Nevertheless, there are some differences between these two types of feedforward controllers.

- (1) The first feedforward controller is the inverse of the feedback control loop, which consists of the controller and the drive, and therefore, it becomes more complicated if a more comprehensive controller (e.g., PID controller) is utilized. Whereas, the latter is the inverse of the drive only, and therefore, the design of its corresponding feedforward controller is simple and independent of the design of the feedback controller.
- (2) If the feedforward controller ( $G_0^{-1}(z)$  in Fig. 5a or  $D_0^{-1}(z)$  in Fig. 5b) includes poles located on or outside the unit circle in the z-domain, the design of the feedforward controller must be modified. The modification of the design in Figure 5a, that will be discussed below, is easier than that in Figure 5b.

In the continuation of this paper, only the first type of feedforward controller is discussed.

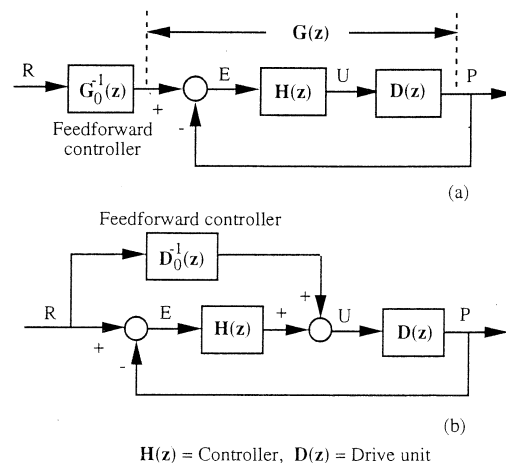


Figure 5: Two principle types of feedforward controllers.

### 4.2 Zero Phase Error Tracking Controller (ZPETC)

A feedforward controller entitled "Zero Phase Error Tracking Controller (ZPETC)" was proposed by Tomizuka [47]. Since we will use this controller as a representative of feedforward controllers, we will elaborate on its principles. The concept of the ZPETC is based on pole/zero cancellation, i.e.,  $G_0^{-1}(z)G(z) = 1$ .

However, if  $G_0^{-1}(z)$  includes unstable poles, it cannot be implemented as a feedforward controller and, therefore, must be modified. Let us assume that the closed-loop discrete-time transfer function, which includes the controlled plant and feedback controller, is expressed as

$$G_{\text{closed}}(z^{-1}) = \frac{z^{-d}B^+(z^{-1})B^-(z^{-1})}{A(z^{-1})} \quad (10)$$

where  $z^{-d}$  represents a delay of  $d$  steps (sampling periods) normally caused by the control loop,  $A$  includes the closed-loop poles,  $B^+$  includes the acceptable closed-loop zeros, and  $B^-$  includes the unacceptable closed-loop zeros. The "acceptable" zeros here mean the zeros that are located inside the unit circle and can be taken as the poles in the feedforward controller. By contrast, unacceptable zeros are located on or outside the unit circle and cannot be the poles of the feedforward controller since they will cause instability. In practical application, a stable zero that is close to the unit circle and is located on or close to the negative real axis (e.g.,  $z = -0.97$ ) may introduce oscillatory mode and, therefore, is regarded as an unacceptable zero.

If unacceptable zeros exist,  $G_0^{-1}(z)$  cannot be implemented in the feedforward controller because it will cause a significant oscillation in the control signals. Tomizuka modified the feedforward controller structure as shown in Figure 6. The modified feedforward controller  $G_f(z)$  has the following form:

$$G_f(z) = \frac{A(z^{-1})B^-(z)}{B^+(z^{-1})[B^-(1)]^2} \quad (11)$$

Multiplying Equations 10 and 11, yields the overall transfer function

$$\frac{P(k)}{R(k+d)} = \frac{B^-(z)B^-(z^{-1})}{[B^-(1)]^2} \quad (12)$$

The frequency transfer function is given by

$$\frac{P(k)}{R(k+d)} = \left[ \frac{B^-(e^{-j\omega})}{B^-(1)} \right] \left[ \frac{B^-(e^{j\omega})}{B^-(1)} \right] \quad (13)$$

Suppose that  $B^-(e^{-j\omega}) = \text{Re} + j\text{Im}$ , where  $\text{Re}$  and  $\text{Im}$  represent the real and imaginary parts respectively, the frequency transfer function becomes

$$\begin{aligned} \left[ \frac{B^-(e^{-j\omega})}{B^-(1)} \right] \left[ \frac{B^-(e^{j\omega})}{B^-(1)} \right] &= \frac{1}{[B^-(1)]^2} [(\text{Re} + j\text{Im})(\text{Re} - j\text{Im})] \\ &= \frac{\text{Re}^2 + \text{Im}^2}{[B^-(1)]^2} \\ &= \left\| \frac{B^-(e^{j\omega})}{B^-(1)} \right\|^2 \end{aligned} \quad (14)$$

As can be seen in Equation 14, the phase angle of the frequency transfer function is zero. Therefore, a zero phase error tracking is provided by the ZPETC method.

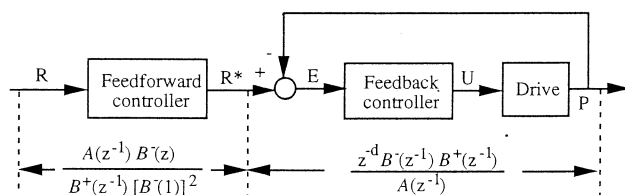


Figure 6: Zero phase error tracking control system.

A zero phase error is achieved by the ZPETC method. The gain error, however, is not eliminated and may cause large tracking errors. Some extra feedforward terms, which can be added to compensate for the gain error, were proposed in [14,51,52].

The major drawback of the ZPETC method is that it requires precise knowledge of the dynamic behavior of the axial drive system. However, there might be a difference between the real drive system and the model used in the computer (i.e., modeling error), and therefore, an additional error source is introduced to the controlled system. Another drawback is that the inverse transfer function in the feedforward controller will cause large control signals (see Section 7.1 below). These signals in practice will be limited by the permissible maximum output of the digital-to-analog converter and the maximum voltage of the motor, and therefore, the performance of the controlled system is degraded.

### 4.3 Inverse Compensation Filter (IKF)

It was found [16,55] that the ZPETC method fails in corner tracking. To remedy this deficiency, Weck proposed [55] an "inverse compensation filter (IKF)" method, which adds a low-pass filter to the feedforward controller and

results in a better performance in corner tracking. The block diagram of the IKF method is shown in Figure 7. The low-pass filter filters out the high-frequency input signals needed in corner tracking and consequently smooths the resultant contouring path.

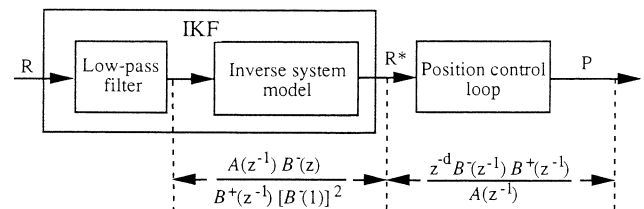


Figure 7: Tracking control system with the inverse compensation filter.

Some other feedforward controllers based on ideas similar to ZPETC and IKF were proposed [14,16,30,40,51,52,54]. They are not discussed here, since their principles are similar.

## 5 CROSS-COUPLING CONTROLLER (CCC)

The cross-coupling control architecture was first proposed by Koren [18]. The main idea of cross-coupling control is to build in real time a contour error model based on the feedback information from all the axes as well as the interpolator, to find an optimal compensating law, and then to feed back correction signals to the individual axes. The cross-coupling controller includes two major parts: (1) the contour error model, and (2) a control law. Consequently, the differences between the various CCCs that were proposed by many other researchers who followed the original work are in the contour error model or in the control law [8,11,22,24-27,31], but all of them are based on the original concept in [18].

A recent version of the CCC, the variable-gain cross-coupling controller proposed by Koren and Lo [22], demonstrated excellent tracking ability on an experimental system and is summarized below. The contour error model is shown in Figure 8. We see that the principle of the CCC is to place the tool P on the contour at point A rather than R, as done with feedback and feedforward controllers. The contour error mathematical model is given in the following equations:

$$\epsilon = -E_x C_x + E_y C_y \quad (15)$$

where  $C_x$  and  $C_y$  are

$$C_x = f(\sin\theta, E_x, \rho) \quad (16)$$

$$C_y = f(\cos\theta, E_y, \rho) \quad (17)$$

where  $\theta$  is the angle between X-axis and the instantaneous tangent to the desired trajectory and  $\rho$  is the instantaneous radius of curvature (Note that  $\rho = \text{constant}$  for a circular contour and  $\rho = \infty$  for a linear contour). The signals  $E_x$  and  $E_y$  are the axial position errors and are measured in real time;  $\theta$  and  $\rho$  are calculated at each sampling period based on the interpolator data.

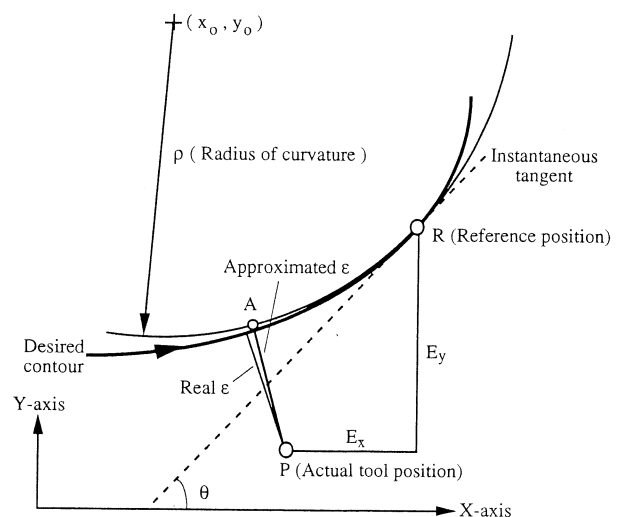


Figure 8: The modeling of the contour error.

Based on the above contour error model, a cross-coupling controller with a PID control law  $W(z) = W_P + W_I \frac{Tz}{z-1} + W_D \frac{z-1}{Tz}$  was implemented on a milling machine and gave error reduction of 5:1 to 10:1 compared with a system with axial P-controllers. A comparison with other controllers is presented below in Section 7. The block diagram of a two-axis cross-coupling control system is shown in Figure 9.

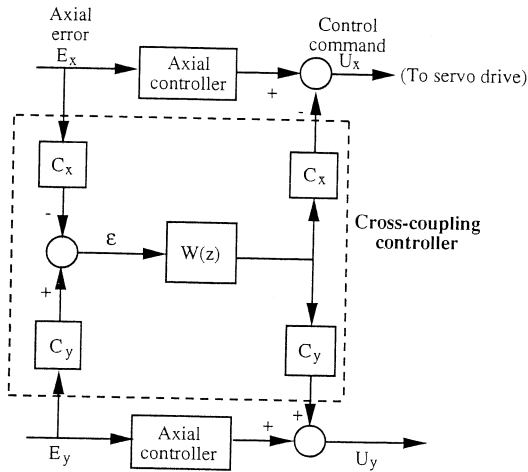


Figure 9: The cross-coupling controller.

## 6 OTHER ALGORITHMS

In addition to the basic three classes discussed above, there are other control algorithms that are discussed in this section.

### 6.1 Optimal Control

The optimal control algorithm can be applied as an efficient controller law of servo-controllers. The principle of the optimal control is minimizing of a performance index subject to the system differential equations. The optimal control has a closed-form solution for a linear system and a quadratic performance index. In machine tool applications if the performance index includes the axial position errors (and their incremental changes), the servo controller becomes a feedback controller [1]. If the contour error is used in the performance index, the servo controller then becomes an optimal cross-coupling controller [25].

### 6.2 Predictive Control

The basic idea of the Generalized Predictive Control (GPC) proposed by Boucher [6] is to make the plant's predicted output coincide with a setpoint or desired known trajectory. Three stages are performed to achieve this goal: (1) first the plant output is predicted, (2) then the future control values that minimize the errors between the predicted outputs and the setpoint values are calculated, and (3) finally only the first optimal control value is applied. The process is iterative and repeated at every sampling period.

The GPC method, however, can be regarded as a particular case of optimal control, in which the performance index includes the errors between the predicted outputs and the desired values.

### 6.3 Adaptive Control

Adaptive control in machining usually means adapting the cutting variable (feed and speed) to the variation in the cutting process [21]. Adaptive control techniques, however, can be applied for completely different purpose - to adjust in real time the parameters of the servo-control loops. It can be used as an accessory algorithm for feedback, feedforward, or cross-coupling controllers.

The feedforward controller is very sensitive to the modeling error and the variations of system parameters. And therefore, an adaptive algorithm is required if the feedforward control approach is applied to machine tool systems [40,42,50].

An adaptive control algorithm can be applied to a mismatched system [33,39]. This adaptive algorithm makes all the individual axial control loops match

artificially and, thereby eliminate the contour error caused by mismatched loop parameters.

In addition, the adaptive control algorithm can also be used as an assistant or parallel algorithm for the cross-coupling controller [11].

## 6.4 Repetitive Control

In addition to the general servo controllers, a special-purpose controller entitled "repetitive" controller may be considered for handling the repetitive tasks with the presence of periodic references and periodic disturbance inputs. Tomizuka proposed a repetitive controller and applied it to a disk-drive system and a turning machine [10,41,42,49,53]. When utilizing a repetitive controller, the axial errors measured when cutting a part are used to compensate the errors in the next part. This algorithm must be applied together with a conventional P-controller [10,49] or other servo-control algorithms (e.g., adaptive ZPETC in [41,42]). It cannot be applied independently and can only be applied to repetitive tasks. Moreover, utilizing the data in previous cuts requires a large memory if a complex part is being machined.

## 7 SIMULATION AND EXPERIMENTAL ANALYSES

The simulations and experiments were performed on a two-axis system. (The block diagram with feedback controllers is shown in Figure 10.) The motor is shown as a first-order model with gain  $K_{mi}$  and time constant  $\tau_i$ ;  $H_x$  and  $H_y$  are the axial controllers;  $K_c$  is the gain of the digital-analog converter;  $K_g$  is the gear ratio,  $K_l$  is the leadscrew pitch, and  $K_e$  is the encoder gain;  $R_x$  and  $R_y$  are the reference positions generated by the interpolator;  $P_x$  and  $P_y$  are the measured positions supplied by the encoders;  $f_x$  and  $f_y$  are the axial velocities;  $E_x$  and  $E_y$  are the axial position errors;  $U_x$  and  $U_y$  are the computer-generated control commands to each moving axis;  $D_x$  and  $D_y$  are the disturbance loads on each axis, resulting from the slide friction and the cutting process forces.

Three basic servo-controllers are analyzed in the following simulations and experiments.

- (1) Feedback controllers: P controller and PID controllers
- (2) Feedforward controllers: ZPETC and IKF
- (3) Cross-coupling controller: variable-gain CCC.

Note that both the feedforward controller and the cross-coupling controller need axial feedback controllers. A P-controller is utilized as the axial feedback controller in the following analyses.

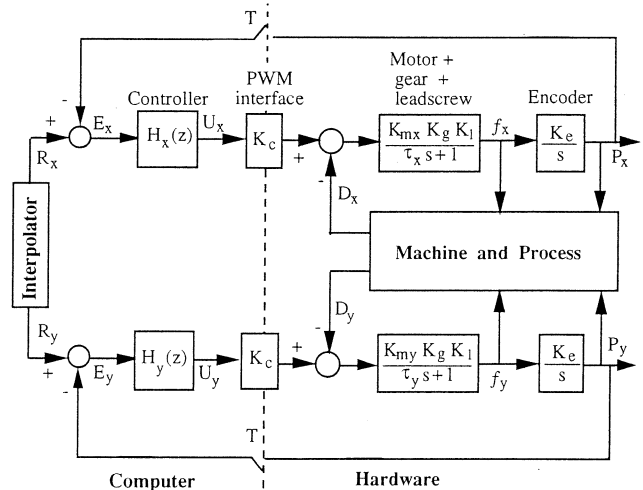


Figure 10: The block diagram of a two-axis machine.

## 7.1 Simulation Analyses

Circular and corner contours were simulated to analyze the controllers' ability to reject different error sources. The system parameters used in the simulations are listed in Table 1.

As was stated above, contour errors due to the control loop structure are caused by three factors: (1) trajectory tracking disability, (2) axis mismatch, and (3) external disturbances. In addition, feedforward controllers have modeling errors and saturation errors.

Table 1: The System Parameters Used in Simulations

Open loop gains: $K_c K_g K_i K_e K_{mx} = 10.0 \text{ s}^{-1}$ , $K_c K_g K_i K_e K_{my} = 10.0 \text{ s}^{-1}$ (= 11.5 $\text{s}^{-1}$ in the mismatched system)
Time constants: $\tau_x = 45 \text{ msec}$ , $\tau_y = 45 \text{ msec}$ (= 65 msec in the mismatched system)
Disturbances: $D_f \approx 100 \text{ bits}$ ( due to friction), $D_c = 160 \text{ bits}$ ( due to cutting force)
$U_{\text{limit}}$ = maximum allowable control command (i.e., saturation)
Controller gains: $K_P = 1$ (for P controller) $K_P = 7, K_I = 50, K_D = 0.5$ (for PID controller) $W_P = 8, W_I = 60, W_D = 0.6$ (for CCC)

**Tracking.** If there are no disturbances and the axial parameters of the axes are identical, the contour error is caused only by trajectory tracking deficiency. Under these conditions (i.e., without disturbances and with matched axial parameters), a circular contour was simulated for different servo-controllers (see Fig. 11). As expected the axial errors of the PID controller were much smaller than those with the P controller (for  $f = 1.88 \text{ m/min}$ , the PID error is within  $\pm 0.35 \text{ mm}$  and the P error is within  $\pm 3.2 \text{ mm}$ ). But surprisingly the contour error with the PID controller is larger than that with the P controller (see Fig. 11). The simulation results show that (1) the PID controller results in poor trajectory tracking (especially for a high angular speed and small radius of curvature), (2) the ZPETC (a feedforward algorithm) can achieve the best tracking performance if there is no modeling error and no disturbances, and (3) the CCC provides a much better tracking ability, compared to P and PID controllers.

**Mismatch.** Under the circumstance of no disturbances, small feedrate, and large mismatch in axial parameters (15% mismatch in open-loop gains and 44% mismatch in time constants), the mismatch of the two axes will dominate the other error sources. Figure 12 shows the simulation results for machining a circular contour under the above circumstances. The results show that all the controllers, except the P-controller, can achieve a very small contour error. If no modeling errors are assured, the feedforward controller (ZPETC) can provide the best tracking performance.

**Modeling error.** Two limitations of the ZPETC method that were not considered in the above simulations are considered here. First, as stated in Section 4, the design of a feedforward controller requires knowledge of the exact model of the drive dynamics. In practice, the control designer does not have a perfect knowledge of the drive model, and the model used in the feedforward controller will be different than the actual drive dynamics. Consequently, the practical system will result in a position error. Figure 13 demonstrates the sensitivity of the ZPETC method to the modeling error. It is shown that even a small modeling error can degrade the tracking performance of the ZPETC method. As compared to the CCC method (which does not require knowledge of plant parameters), ZPETC can provide a better tracking performance only when the modeling error is less than 0.5%. This limitation, however, is not realistic. Modeling errors of 2% to 5% or even higher in some parameters are more realistic.

**Saturation.** The other limitation of the ZPETC method is the saturation of the control commands that the computer generates. For proper operation, the ZPETC method needs a very large control command in the transient state to overcome the axial error caused by the drive inertia. The large control command will saturate in a practical CNC system. Figure 14 depicts the influence of saturation constraints in the computer output on the ZPETC and CCC methods. In our system, the computer output  $U$  is a binary word sent to the PWM amplifier. For example, if the output line has 8 bits, the command is limited to -128 to +127, and a command exceeding the above limitation will be truncated. As can be seen in the simulation results, the ZPETC is strongly limited by the the saturation constraint.

By contrast, the CCC, P, and PID controllers are usually not influenced by the saturation constraints.

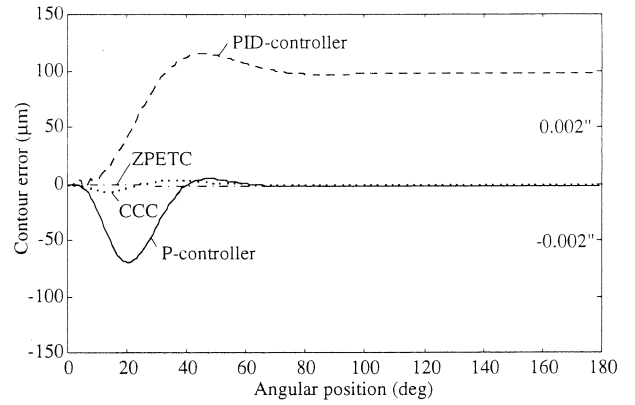


Figure 11: Examining tracking ability by simulation of a circular motion for different servo-controllers. Conditions: Feedrate = 1.88 m/min (= 74 ipm). Radius of circle = 20 mm (= 0.79 inch). No disturbances, no mismatch in axial parameters. No modeling error in ZPETC.

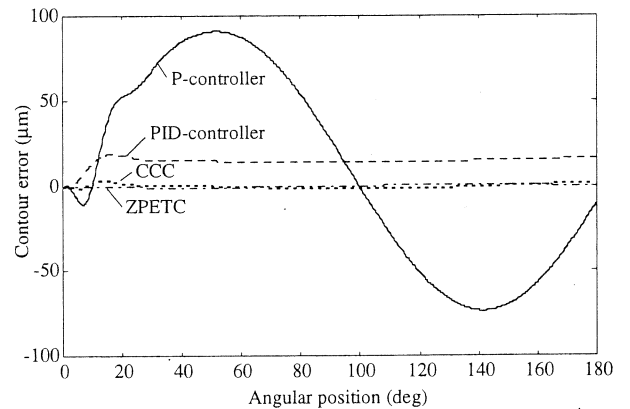


Figure 12: Examining the effect of mismatch in axial parameters by simulation of a circular motion for different servo-controllers. Conditions: Feedrate = 0.754 m/min (= 29.7 ipm). Radius of circle = 20 mm. No disturbances. No modeling error in ZPETC.

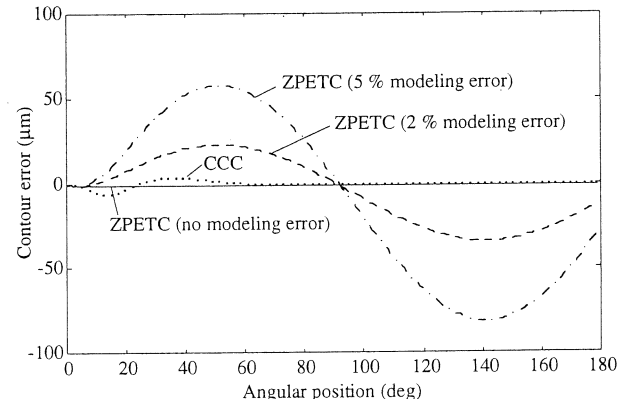


Figure 13: The effect of modeling error on ZPETC method (simulation of a circular motion). Conditions: Feedrate = 0.754 m/min (= 29.7 ipm). Radius of circle = 20 mm. No disturbances. No mismatch in axial parameters.

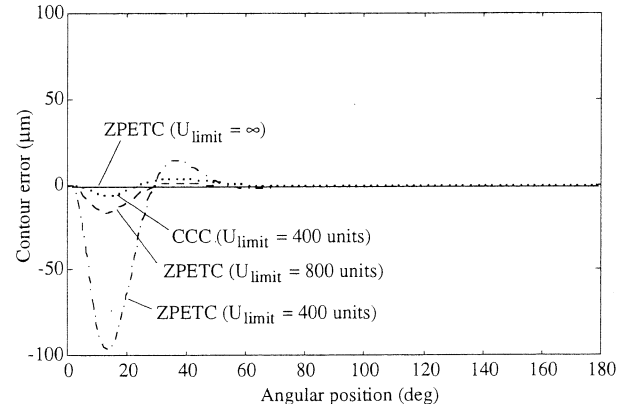


Figure 14: The effect of saturation on performance (simulation of a circular motion). Conditions: Feedrate = 0.754 m/min (= 29.7 ipm). Radius of circle = 20 mm. No disturbances, no mismatch in axial parameters. No modeling error in ZPETC

**Disturbances.** Figures 15 and 16 show the disturbance rejection ability for each of the four control algorithms. The simulation in Figure 15 considers only the friction in the table guide-ways and that in Figure 16 considers only the effect of the cutting force (see Equations 3 and 4). Both simulation results show that (1) the CCC and PID controller have a good ability in disturbance rejection (CCC is the best), and (2) P controller and ZPETC have very poor performances in disturbance rejection. (To achieve a good disturbance rejection, the ZPETC should be combined with a properly designed feedback controller. Only then it can work in a realistic environment.)

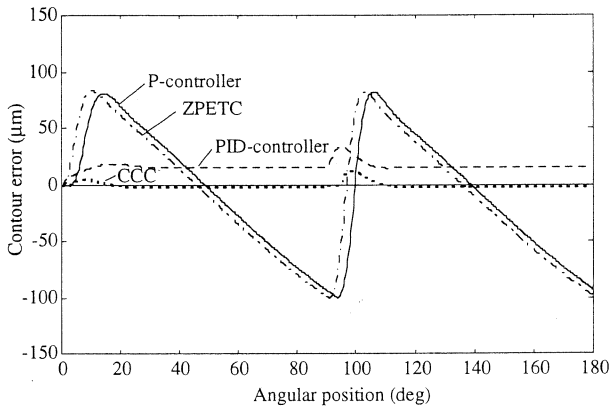


Figure 15: Rejection ability of friction disturbance (simulation of a circular motion for different servo-controllers). Conditions: Feedrate = 0.754 m/min (= 29.7 ipm). Radius of circle = 20 mm. No mismatch in axial parameters. No modeling error in ZPETC.

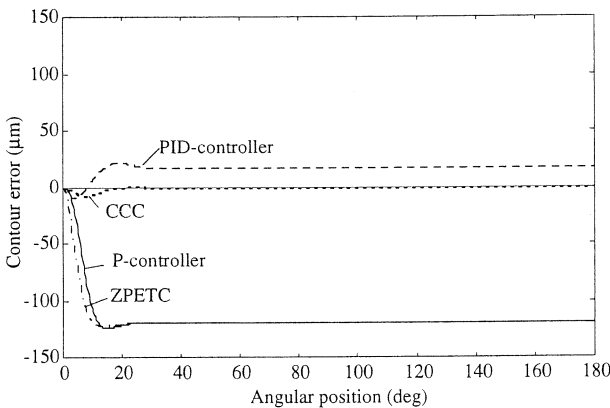


Figure 16: Rejection ability of cutting force disturbance (simulation of a circular motion for different servo-controllers). Conditions: Feedrate = 0.754 m/min (= 29.7 ipm). Radius of circle = 20 mm. No mismatch in axial parameters. No modeling error in ZPETC.

**Corners.** Corner tracking is a special, but important case in contouring applications. Corner tracking has been simulated with each control algorithm (see Fig. 17). The results show that (1) a P controller can provide average quality in corner tracking, (2) a basic PID controller results in a significant overshoot at the corner, (3) both ZPETC and CCC methods can provide good accuracy in tracking a corner. The ZPETC method, however, can provide good corner tracking only under the conditions of very small modeling error and no saturation constraint; both conditions are impractical in most systems. As can be seen in Figure 18, the ZPETC method fails at corner tracking due to the saturation limitation. As stated in Section 4, the IKF method, in which a low-pass filter precedes the feedforward controller, can be used to provide a better performance in corner tracking. The simulation results in Figure 18 prove the effectiveness of the IKF method. The IKF method, however, cannot provide a good performance with a significant modeling error.

## 7.2 Experimental Analyses

The experimental tests were conducted on a 3HP two-axis milling machine, the system parameters of which are listed in Table 2. The machine was interfaced with our computer, which allows us to write our own control software and test it on this real system. As can be seen in Table 2, this machine has the following characteristics: (1) small mismatch in axial parameters, (2) high friction loads, and (3) low maximum feedrate limitation. According to the simulation analyses, we may expect that only the CCC and PID controllers can perform well because of the large friction disturbances existing on this machine. For this paper, linear and circular motions were tested on this CNC system and the experimental results (shown in Figures 19 and 20) confirm this expectation.

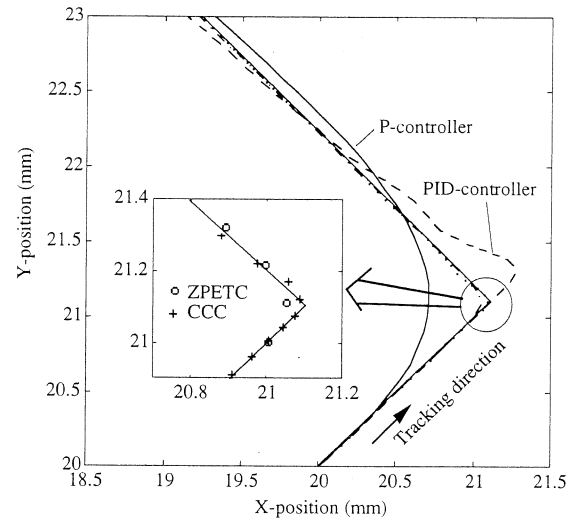


Figure 17: Simulation of a corner motion for different servo-controllers. Conditions: Feedrate = 0.9 m/min (= 35.4 ipm). No disturbances, no mismatch in axial parameters. No modeling error in ZPETC.

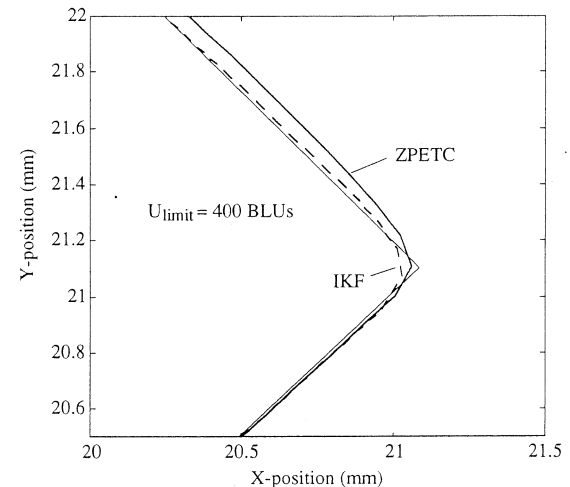


Figure 18: Examining the effect of saturation on ZPETC and IKF methods by simulation of a corner motion. Conditions: Feedrate = 0.9 m/min (= 35.4 ipm). No disturbances, no mismatch in axial parameters. No modeling errors.

Table 2: The Parameters of the Experimental System

$K_g = \frac{10}{32}$ ,	$K_I = 5.08 \text{ mm (0.2 inch)}$ ,	$K_e = 100 \text{ pulses/mm}$
$K_c K_{mx} = 0.181 \text{ rev/(sec-bit)}$ ,	$K_c K_{my} = 0.185 \text{ rev/(sec-bit)}$	
$\tau_x = 44 \text{ msec}$ ,	$\tau_y = 47 \text{ msec}$	
$D_f = 12.0 \text{ bit (for X-axis)}$ ,	$D_f = 13.5 \text{ bit (For Y-axis)}$	
$U_{limit} = 127 \text{ bits (} f_{max} = 2 \text{ m/min)}$ ,	$BLU = 0.01 \text{ mm}$ .	

As can be seen in Figure 19, the ZPETC method results in the worst performance in linear cuts. The ZPETC, as well as the P controller, cannot provide a good disturbance rejection ability (see Section 7.1). Moreover, the ZPETC results in an additional error due to the modeling error, which doesn't exist with a P controller. As expected, the advantage of the ZPETC is its ability in tracking nonlinear contours such as circles, rather than linear contours. The PID controller, as can be seen in Figure 19, results in a significant overshoot at the transient state (without programmed acceleration). In addition, it also causes large overshoots at the end of the cuts (for both linear and circular cuts). To remedy this drawback, pre-programming of acceleration and deceleration periods is required, whereas they are not needed with CCC, P, and ZPETC methods. Adding acceleration and deceleration periods will increase the cutting time. Overall, the CCC method provides the best performance in both linear and circular cuts.

A circular motion with a higher feedrate (1.5 m/min) has also been tested on the milling system (see Figure 21). According to Equation 6, the increase in the feedrate makes the contour error due to trajectory tracking more significant. At high feedrates, the PID controller failed; it cannot provide good tracking. The

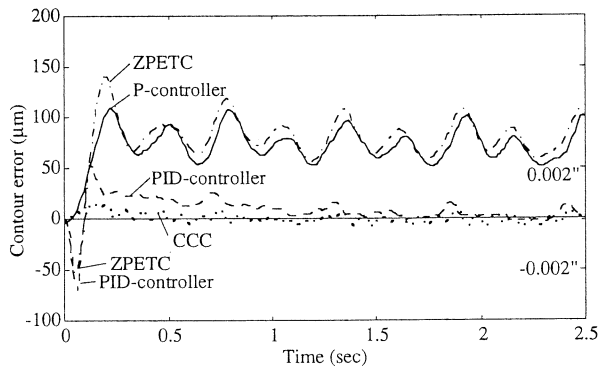


Figure 19: Experimental results of a straight-line motion for different servo-controllers. Conditions: Feedrate = 1.2 m/min (= 47.2 ipm). Angle between straight line and the X-axis = 26.6°.

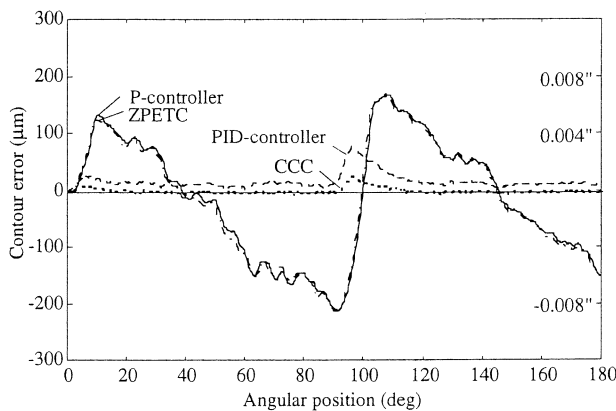


Figure 20: Experimental results of a circular motion for different servo-controllers. Conditions: Feedrate = 0.377 m/min (= 14.8 ipm). Radius of circle = 20 mm.

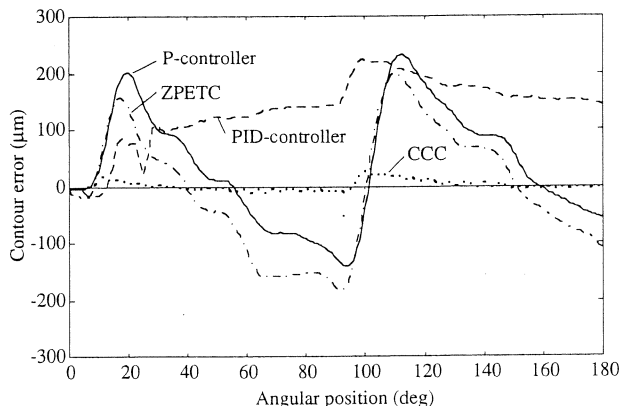


Figure 21: Experimental results of a circular motion for different servo-controllers. Conditions: Feedrate = 1.51 m/min (= 59.4 ipm). Radius of circle = 20 mm.

ZPETC method provides better tracking compared to the P and PID controllers. (Note that the ZPETC method is expected to provide much better tracking performance than P and PID controllers, when a relatively high feedrate, e.g., 10 m/min, is utilized.) Nevertheless, the CCC is the only method that can provide a small contour error under such circumstances.

## 8 CONCLUSIONS AND FUTURE DIRECTIONS

Existing servo-controllers for contouring applications have been classified and tested in this paper. The control algorithms have been grouped into three basic classes and have been analyzed through simulations and experiments. According to the simulations and experimental results, a comparison of these servo-controllers is summarized in Table 3.

Based on the comparison, the selection of servo-controllers for different machine tool contouring applications and cutting conditions is suggested in the following:

- (1) The P controller works well only when cutting a contour on a machine with small friction, small cutting loads, small mismatch in axial parameters, and conventional feedrates (e.g., 0.25 m/min = 10 ipm).
- (2) The PID controller has a good disturbance rejection ability and is more robust to mismatched axial parameters. Its drawbacks are poor tracking ability of nonlinear contours and sharp corners, and in addition, it may result in an overshoot at stopping. Therefore, the PID controller is preferred on low-speed machines. Usually, a deceleration is needed at the end of every contour segment in order to avoid the overshooting problem. However, this increases the total cutting time. A special algorithm can be utilized to perform corner tracking: the I component of the PID controller can be turned off before the corner. This, however, can cause undercut and contour errors because of the friction and other disturbances.
- (3) The ZPETC and IKF methods are preferred when cutting nonlinear contours at high-speed machining if the system model is well known and no varying or nonlinear characteristics exist. In addition, a properly designed feedback controller is needed to provide the disturbance rejection ability.
- (4) The CCC method provides a good contouring accuracy under any condition and, therefore, is the best choice for a servo-control algorithm. Its drawback, however, is a higher computation load, since in addition to the conventional servo loop algorithm it has to also run the CCC algorithm. With the existing computation power (e.g., INTEL-80486) this does not impose a limitation on a 3-axis system, but deteriorates the performance of 5-axis systems. Nevertheless, with the increase in computation speed of microprocessors, this drawback will shortly disappear.

Table 3: The Evaluation of Servo-Controllers

	P control	PID control	Feedforward (with P controller)	CCC
Tracking nonlinear trajectories	Fair	Fair (low f) Poor (high f)	Excellent (1) Fair (2)	Good
Sharp corners	Fair	Poor	ZPETC: Fair (1,2) IKF: Excellent (1) Fair (2)	Excellent
Axis mismatch	Fair	Good	Excellent (1) Fair (2)	Excellent
Disturbances:	Poor	Good	Poor	Excellent
(b) Cutting force	Poor	Good	Poor	Excellent
Special problems		Overshoot at stopping	Performance is sensitive to modeling error and saturation	Requires a fast processor

Comments:

1. Assume no difference between theoretical model and real system.
2. Assume 2% difference between theoretical model and real system.  $f$  = feedrate

Grading: Excellent, Good, Fair, Poor

In addition to the basic control approaches, some other modified methods may also be considered as algorithms for servo-controllers. They are summarized



below:

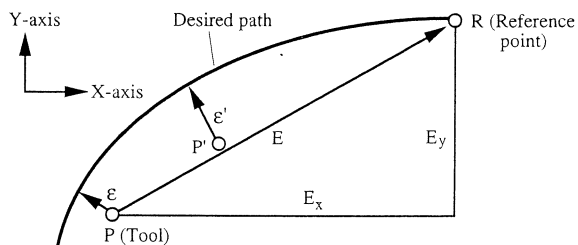
- (1) An adaptive algorithm can be added to a ZPETC method to cope with the modeling error and parameter variation. If the adaptive algorithm utilizes parameter estimation, it may be limited by the richness of the input signals. (The most popular contours in machine tools are lines and circles, which enable us to estimate accurately a second-order closed-loop system.) Therefore, a careful design of the adaptive algorithm is required if the closed-loop system includes higher order structure.
- (2) A combined algorithm of PID control and ZPETC may have the ability to reject all the error sources (see Table 3), because of the ZPETC ability in trajectory tracking and the PID control in disturbance rejection. However, a deceleration at end of each contour is needed for reducing the overshooting caused by PID control.
- (3) A combined algorithm of the CCC and the feedforward controller, which is suggested in Figure 5b, can reject all the error sources without causing the overshooting (see Table 3).

Based on the above analyses and discussions, combinations of the three types of servo-controllers for different environments are suggested. For example, a combined algorithm of the cross-coupling controller and the feedforward controller (with a small modeling error) is suggested for tracking a nonlinear contour at high feedrates (see Figure 23).

An important direction in future servo-controllers will be a design to accommodate high-speed machining, which, in turn, requires minimizing contour errors during transient periods rather than steady-state. High-speed machining requires a proportional increase in the axial velocities. Therefore, for a certain transient period, the *transient distance* increases in proportion to speed. For example, if the transient period is 0.1 sec and the feedrate is 0.3 m/min (= 12 ipm), the transient period is 0.5 mm. However, if the feedrate is increased by 40 times to 12 m/min, the transient distance becomes 20 mm (0.8 inch). That means that the entire cutting will be performed during transients, which requires new control design.

Another direction in future servo-controllers will be a design to accommodate precision machining of complex part surfaces. Machining of complex part surfaces keeps increasing for the following reasons: (1) the trend toward near-net-shape manufacturing requires complex dies and (2) simplified assembly calls for fewer but more complex parts.

To cope with the above two trends, future position servo-drives for machine tools will be based on a combination of the cross-coupling control and the feedforward control. As shown in Figure 22, the concept of the cross-coupling control is that the tool has to be in the *right place*, i.e., minimizing the contour errors. By contrast, traditional and feedforward controllers are based on the strategies of bringing the tool to the reference at the *right time*. Note that without the cross-coupling controller, reducing the axial errors, which is the objective of the axial feedback and the feedforward controllers, does not necessarily reduce the contour error. For example, as can be seen in Figure 22, the tool is brought closer to the reference point (from P to P'). This, however, results in a larger contour error ( $\epsilon < \epsilon'$ ). Therefore, the core of the servo-drive feed control will be the cross-coupling controller, but it will be augmented by feedforward algorithms such as ZPETC or IKF, which are strongly recommended for nonlinear cuts at high feedrates (see Figure 23). This combination will minimize the contour error with a minimum time lag between reference command and the actual tool position. The concept of this future combined controller will be to bring the tool to the *right place at the right time*.



CCC objective: Reduce  $\epsilon$   
 Feedback & Feedforward objectives: Reduce E by reducing  $E_x$  and  $E_y$

Figure 22: Controller objectives of the CCC, feedback, and feedforward controllers.

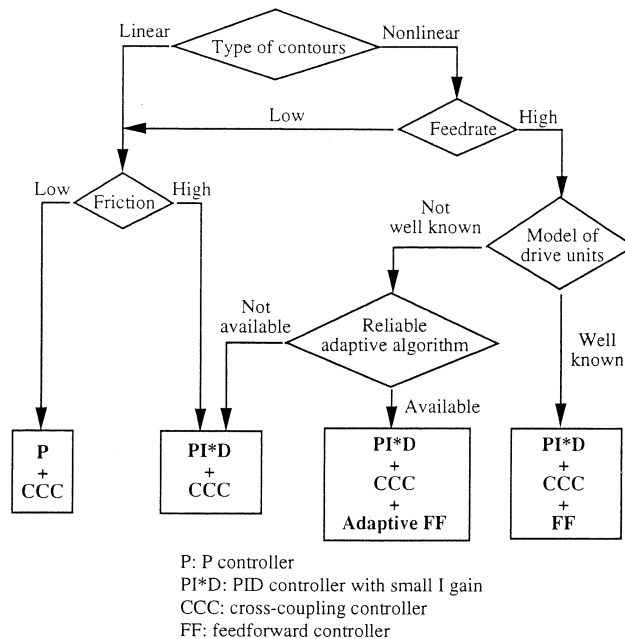


Figure 23: Suggested combinations for the servo-controllers.

An additional direction of the design of servo-control algorithms will be a flexible selection of the combined controllers according to the variations of the environments such as types of contours, modeling knowledge, feedrates, etc. (See Figure 23)

As stated in Section 2, the error sources caused by the hardware deficiencies (e.g., backlash, geometric errors) and the cutting process effects (e.g., thermal error, tool wear) cannot be reduced by the control techniques discussed in this paper. Therefore, in addition to the servo-control algorithm, compensation techniques for the backlash, tool wear, friction, thermal and geometric errors, etc. will be introduced as an accessory algorithm in future CNC systems.

#### Acknowledgements

The following CIRP colleagues contributed to this paper: P. Boucher, H. Makino, H. B. Roelofs, H. K. Tönshoff, M. Weck, and K. Yamazaki. We especially appreciate the contributions of Professors G. Pritschow, M. Tomizuka, A. G. Ulsoy, and H. Van Brussel; each of them sent a few pages with comments on the original draft that substantially improved the quality of this paper.

Parts of this research have been supported by the NSF Industry/University Research Center at the University of Michigan and by NSF grant # DDM-9114131.

#### 9 REFERENCES

- [1] Astrom, K. J. and Wittenmark, B., 1984, *Computer Controlled Systems: Theory and Design*, Prentice-Hall, Inc.
- [2] Astrom, K. J. and Wittenmark, B., 1989, *Adaptive Control*, Addison-Wesley Publishing Company.
- [3] Ber, A., Rotberg, J., and Zombach, S., 1988, "A Method for Cutting Force Evaluation of End Mills," *Annals of the CIRP*, Vol. 37/1/88, pp. 37-40.
- [4] Bin, H. Z., Yamazaki, K., and DeVries, M. F., 1983, "A Microprocessor-Based Control Scheme for the Improvement of Contouring Accuracy," *Annals of the CIRP*, Vol. 32/1/83, pp. 275-279.
- [5] Boucher, P., Dumur, D., Kapusta, Z., and Duchaine, P. J., 1989, "Improvement of Productivity with Predictive Control in Speed and Position," *Annals of the CIRP*, Vol. 38/1/89, Aug, pp. 339-342.
- [6] Boucher, P., Dumur, D., and Faissal Rahmani, K., 1990, "Generalized Predictive Cascade Control (G.P.C.C.) for Machine Tool Drives," *Annals of the CIRP*, Vol. 39/1/90, Aug, pp. 357-360.
- [7] Boucher, P., Dumur, D., and Daumuller, S., 1991, "Predictive Cascade Control of Machine Tools Motor Drives," *Proceeding EPE 91*, Florence, Vol. 2, Sep., pp. 120-125.
- [8] Burhoe, J. C. and Nwokah, O. D., 1989, "Multivariable Control of a Biaxial Machine Tool," *Proceedings of the Symposium on Dynamic Systems, Measurement, and Control*, ASME Winter Annual Meeting, San Francisco, California, Dec., pp. 1-6.

- [9] Canudas, C., Astrom, K. J., and Braun, K., 1986, "Adaptive Friction Compensation in DC Motor Drives," *Proceedings of the 1986 IEEE International Conference on Robotics and Automation*, San Francisco, April, pp. 1556-1561.
- [10] Chew, K. K. and Tomizuka, M., 1990, "Steady-State and Stochastic Performance of a Modified Discrete-Time Prototype Repetitive Controller," *ASME Transaction, Journal of Dynamic Systems, Measurement and Control*, Vol. 112, March, pp. 35-41.
- [11] Chuang, H. Y. and Liu, C. H., 1991, "Cross-Coupled Adaptive Feedrate Control for Multi-axis Machine Tools," *ASME Transaction, Journal of Dynamic Systems, Measurement and Control*, Vol. 113, September, pp. 451-457.
- [12] Doraiswami, R. and Gulliver, A., 1984, "A Control Strategy for Computer Numerical Control Machine Exhibiting Precision and Rapidity," *Trans. of ASME, Journal of Dynamic Systems, Measurement and Control*, Vol. 106, pp. 56-62.
- [13] Faissal Rahmani, K., Dumur, D., and Boucher, P., 1990, "Generalized Predictive Control with Multiple Reference Model (G.P.C./M.R.M.) for Self-Synchronous Motors," *Proc. IMACS TC1'90*, Nancy, September, Vol. 1, pp. 9-14.
- [14] Haack, B. and Tomizuka, M., 1991, "The Effect of Adding Zeros to Feedforward Controllers," *ASME Transactions, Journal of Dynamic systems, Measurement, and Control*, Vol. 113, March, pp. 6-10.
- [15] Johnson, W. C., Shrinivasan, K. and Kulkarni, P., 1984, "Digital Control Algorithms for Electrical Machine Tool Feed Drives," *Proceedings of the 12th North American Manufacturing Research Conference*, Houghton, Michigan, pp. 447-453.
- [16] Jouaneh, M., Wang, Z., and Dornfeld, D., 1988, "Tracking of Sharp Corners Using A Robot and A Table Manipulator." University of California, Berkely, Beitrag für das U.S.A.-Japaaan Symposium on Flexible Automation, July.
- [17] Koren, Y., 1979, "Design of Computer Control for Manufacturing Systems," *ASME Transaction, Journal of Engineering for Industry*, Vol. 101, No. 3, August, pp. 326-332.
- [18] Koren, Y., 1980, "Cross-Coupled Biaxial Computer Control for Manufacturing Systems," *ASME Transaction, Journal of Dynamic Systems, Measurement and Control*, Vol. 102, No. 4, December, pp. 265-272.
- [19] Koren, Y., 1983, *Computer Control of Manufacturing Systems*, McGraw-Hill, New York.
- [20] Koren, Y., 1985, *Robotics for Engineers*, McGraw-Hill, New York.
- [21] Koren, Y., 1989, "Adaptive Control Systems for Machining," *Manufacturing Review*, Vol. 2, No. 1, March, pp. 6-15.
- [22] Koren, Y. and Lo, C. C., 1991, "Variable-Gain Cross-Coupling Controller for Contouring," *Annals of the CIRP*, Vol. 104, Aug., pp. 371-374.
- [23] Kronenberg, M., 1966, *Machining Science and Application*, Pergamon Press.
- [24] Kulkarni, P. K. and Srinivasan, K., 1986, "Cross-Coupled Controller for Multi-Axial Drive Servomechanisms," *Proceedings of the Japan-USA Symposium on Flexible automation*, pp. 585-594, Osaka, Japan. July 14-18.
- [25] Kulkarni, P. K. and Srinivasan, K., 1989, "Optimal Contouring Control of Multi-Axis Drive Servomechanisms," *ASME Transaction, Journal of Engineering for Industry*, Vol. 111, May, pp. 140-148.
- [26] Kulkarni, P.K. and Srinivasan, K., 1990, "Cross-Coupled Control of Biaxial Feed Drive Servomechanisms," *ASME Transactions, Journal of Dynamic systems, Measurement and Control*, Vol. 112, No. 2, June, pp. 225-232.
- [27] Liu, C. H. and Chan, W. M., 1985, "Microprocessor-Based Cross-Coupled Biaxial Controller for A Two-Axis Positioning System," *IEEE transactions, Journal of Industrial Electronics and Control Instrumentation*, pp. 327-332.
- [28] Makino, H. and Ohde, T., 1991, "Motion Control of the Direct Drive Actuator," *Annals of the CIRP*, Vol. 40/1/1991, pp. 375-378.
- [29] Markiewicz, B. R., 1973, "Analysis of Computed Torque Drive Method and Comparison with Conventional Position Servo for a Computer-Controlled Manipulator," *NASA Tech, Memo 33-601*, J. P. L.
- [30] Masory, O., 1985, "The Effect of a Velocity Feed Forward Loop on Contour Accuracy," *Proceedings of 7th International Motor Conference*, October, pp. 418-428.
- [31] Masory, O. and Wang, J., 1991, "Improving Contouring system Accuracy by Two-stage Actuation," *NAMRC Proceedings*.
- [32] Ono, Y. and Kuwahara, H., 1986, "The New Design of Motor, Position Sensor and Position Control System for Direct Drive Manipulators," *ASME Proceedings, Robotics: Theory and Applications*, Anaheim, California, December, pp. 123-128.
- [33] Pak, H. A., 1991, "Adaptive Matching and Preview Controllers for Feed Drive Systems," *ASME Transaction, Journal of Dynamic Systems, Measurement and Control*, Vol. 113, June, pp. 316-320.
- [34] Paul, R. P., 1981, *Robot Manipulators: Mathematics, Programming, and Control*, MIT press, Cambridge, Mass.
- [35] Poo, A., Bollinger, J. G., and Younkin, W., 1972, "Dynamic Errors in Type I Contouring Systems," *IEEE Transaction on Industrial Applications*, Vol. IA-8, No. 4, pp. 477-484.
- [36] Pritschow, G. and Philipp, W., 1990, "Direct Drives for High-Dynamic Machine Tool Axes," *Annals of the CIRP*, Vol. 39/1/1990, pp. 413-416.
- [37] Schepper, F. and Yamazaki, K., 1988, "Application of ASIC-Techonology to Mechatronics Control: Development of the Flexible Servo Peripheral Chip," *Annals of the CIRP*, Vol. 37/1/1988, pp. 389-392.
- [38] Schepper, F. and Yamazaki, K., 1989, "Development of an ASIC Performing High Speed Current Loop Processing of Servo Motor Control for Mechatronics Applications," *Annals of the CIRP*, Vol. 38/1/1989, pp. 355-358.
- [39] Tabrizi-Hagi, S., 1992, "Real-Time Adjustment of Non-Traditional Machining Parameter in CNC," Ph. D. Dissertation, the University of Michigan.
- [40] Tsao, T.C. and Tomizuka, M., 1987, "Adaptive Zero Phase Error Tracking Algorithm for Digital Control," *ASME Transaction, Journal of Dynamic Systems, Measurement and Control*, Vol. 109, December, pp. 349-354.
- [41] Taso, T. C. and Tomizuka, M., 1988, "Adaptive and Repetitive Control Algorithms for Noncircular Machining," *Proceedings of the 1988 American Control Conference*, June, pp. 115-120.
- [42] Taso, T. C. and Tomizuka, M., 1988, "Hydraulic Servo System Design for Noncircular Machining," *Proceedings of the 1988 NAMRC*, Illinois, May, pp. 336-343.
- [43] Tomizuka, M., Dornfeld, D., and Purcell, M., 1980, "Application of Microcomputers to Automatic Weld Quality Control," *ASME Transactions, Journal of Dynamic systems, Measurement, and Control*, Vol. 102, June, pp. 62-68.
- [44] Tomizuka, M., 1984, "Experimental Evaluation of the Preview Servo Scheme for a Two-Axis Position System," *ASME Transactions, Journal of Dynamic systems, Measurement, and Control*, Vol. 106, March, pp. 1-5.
- [45] Tomizuka, M., Dornfeld, D., Chen, M. S., and Taso, T. C., 1986, "Noncircular Cutting with Lathe," *Proceedings of the 14th North American Manufacturing Research Conference*, May, pp. 201-206.
- [46] Tomizuka, M., Chen, M. S., Renn, S., and Taso, T. C., 1987, "Tool positioning for Noncircular Cutting with Lath," *ASME transaction, Journal of Dynamic systems, Measurement, and Control*, Vol. 109, June, pp. 176-179.
- [47] Tomizuka, M., 1987, "Zero Phase Error Tracking Algorithm for Digital Control," *ASME Transactions, Journal of Dynamic systems, Measurement, and Control*, Vol. 109, March, pp. 65-68.
- [48] Tomizuka, M., 1988, "Design of Digital Tracking Controllers for Manufacturing Applications," *Control methods for Manufacturing Processes*, DSC-Vol. 9, December, pp. 71-78. (Also in *Manufacturing Review*, Vol. 2, No. 2, pp. 82-90, June 1989)
- [49] Tomizuka, M., Taso, T. C., and Chew, K. K., 1989, "Analysis and Synthesis of Discrete-Time Repetitive Controllers," *ASME Transaction, Journal of Dynamic Systems, Measurement and Control*, Vol. 111, September, pp. 353-358.
- [50] Tomizuka, M., 1990, "Synchronization of Two Motion Control Axes Under Adaptive Feedforward Control," *Adaptive and Learning Control*, DSC-Vol. 21, pp. 1-8.
- [51] Torfs, D., Swevers, J., De Schutter, J., 1991, "Quasi-Perfect Tracking Control of Non-Minimal Phase Systems," *Proceedings of the 30th IEEE Conference on Decision and Control*, Brighton, U. K.
- [52] Torfs, D., De Schutter, J., and Swevers, J., 1992, "Extended Bandwidth Zero Phase Error Tracking Control of Non-Minimal Phase Systems," *ASME Transaction, Journal of Dynamic Systems, Measurement and Control*, Vol. 114, September.
- [53] Tung, E., Anwar, G., and Tomizuka, M., 1991, "Low Velocity Friction Compensation and Feedforward Solution Based on Repetitive Control," *Proceedings of the 1991 American Control Conference*, June, pp. 2615-2620.
- [54] Weck, M. and Ye, G., 1987, "Smooth Motion Control of Automated Industrial Processes," *10th World Congress on Automatic Control*, "Vol. 4, Subject Area 8.1 - 3, pp. 186-191, München, July.
- [55] Weck, M. and Ye, G., 1990, "Sharp Corner Tracking Using the IKF Control Strategy," *Annals of the CIRP*, Vol. 39/1/1990, pp. 437-441.
- [56] Yamazaki, K., 1987, "Development of Flexible Actuator Controller for Advanced Machine Tool and Robot Control," *Annals of the CIRP*, Vol. 36/1/1987/, pp. 285-288.